Continuous Crystalline Carbonate Apatite Thin Films. A Biomimetic Approach

Guofeng Xu,[§,†] Ilhan A. Aksay,[‡,†] and John T. Groves*[,§,†]

Contribution from the Departments of Chemistry and Chemical Engineering, Princeton Materials Institute, Princeton University, Princeton, New Jersey 08544

Received July 12, 2000

Abstract: In contrast to extensive studies on hydroxyapatite thin films, very little has been reported on the thin films of carbonated apatite (dahllite). In this report, we describe the synthesis and characterization of a highly crystalline dahllite thin film assembled via a biomimetic pathway. A free-standing continuous precursor film of carbonated calcium phosphate in an amorphous phase was first prepared by a solution-inhibited templating method (template-inhibition) at an air−water interface. A stearic acid surface monolayer acted as the template, while a carbonate−phosphate solution composed a binary inhibition system. The precursor film formed at the air/water interface was heated at 900 °C and transformed into a dense crystalline film that retained the overall shape of the precursor. The crystalline phase was characterized by XRD and IR to be a single-phase carbonate apatite, with carbonate substitutions in both type A (OH^-) and type B (PO_4^{3-}) lattice positions.

Introduction

Due to its importance in biomedical research, hydroxyapatite has been subjected to extensive studies.[1] In particular, much interest has been drawn to studies of hydroxyapatite thin films for the obvious reason that they are good candidates as bioactive coatings for bone implants.[2] By contrast, much less effort has been devoted to the synthesis and characterization of thin films of carbonated hydroxyapatite (dahllite). This is surprising, considering the fact that dahllite is more closely related to biological apatite than hydroxyapatite and a number of studies have been done on the bulk properties of carbonated apatite.[1,3−5]

Carbonated apatite constitutes the inorganic components of enamel, dentine, and bone, and has a carbonate concentration in the range of a few percent by weight.[1,3] The incorporation of carbonate into apatite structure can influence the structure[6,7] as well as the morphology[8] of the apatite and is thought to alter the biological reactivity of the bone mineral.[9−12] Carbonated apatite is regarded as a better model for bone minerals[1] and, therefore, carbonated apatite thin film coatings are likely to be more biologically compatible.[13] Thus, it is important to study the properties of thin films made of carbonated apatite as well.

The lack of reports on carbonate apatite thin films may be attributed to the under-development of proper synthetic methods that are geared to carbonated apatite. A number of synthetic methods have been developed to prepare hydroxyapatite ($(Ca_{10}(PO_4)_6(OH)_2$) thin films with a variety of thicknesses, porosity, and structure.[1,2] The preparation techniques range from dry physical techniques[1,2,14] to wet chemical routes.[1,2,15−20] The dry physical techniques such as plasma spraying and sputter coating often require high temperature and high vacuum.[1,15] It is not apparent that these methods can be readily adapted to the synthesis of carbonate apatite thin films since carbonate tends to decompose under such conditions. In addition, if the objects to be coated are large or irregularly shaped, the complexity of equipment required could be a practical problem. Wet chemical routes can offer some alternative solutions.[15,18,21] However, many films synthesized in solution are poorly crystalline[16,17,22] and/or discontinuous with porous patches.[23,24] Therefore, much

* To whom inquiries should be addressed.
§ Department of Chemistry.
† Princeton Materials Institute.
‡ Department of Chemical Engineering.

(1) Elliot, J. C. *Structure and Chemistry of The Apatites and The Other Calcium Orthophosphates*; Elsevier Science B.V.: Amsterdam, 1994.
(2) Heimann, R. B.; Vu, T. A.; Wayman, M. L. *Eur. J. Miner.* **1997**, *9*, 597.
(3) Driessens, F. C. M.; Verbeeck, R. M. H. *Biominerals*; CRC Press: Boca Raton, FL, 1990.
(4) Bonel, G. *Ann. Chim.* **1972**, *7*, 127.
(5) Bonel, G. *Ann. Chim.* **1972**, *7*, 65.
(6) Zapanta-Legeros, R. *Nature* **1965**, *206*, 403.
(7) Legeros, R. Z.; Trautz, O. R.; Legeros, J. P.; Klein, E. *Bull. Soc. Chim. Fr.* **1968**, 1712.
(8) Legeros, R. Z.; Trautz, O. R.; Legeros, J. P.; Klein, E. *Science* **1968**, *155*, 1409.
(9) Nelson, D. G. A. *J. Dent. Res.* **1981**, *60* (C), 1621.
(10) Nelson, D. G. A.; Featherstone, J. D. B.; Duncan, J. F.; Cutress, T. W. *Caries Res.* **1983**, *17*, 200.
(11) Blumenthal, N. C.; Betts, F.; Posner, A. S. *Calcif. Tiss. Res.* **1975**, *18*, 81.
(12) Baig, A.; Fox, J.; Hsu, J.; Wang, Z.; Otsuka, M.; Higuchi, W. I.; Legeros, R. Z. *J. Colloid Interface Sci.* **1996**, *179*, 608.
(13) Ellies, L. G.; Nelson, D. G. A.; Featherstone, J. D. B. *J. Biomed. Mater. Res.* **1988**, *22*, 541.
(14) Fernandez-Pradas, J. M.; Sardin, G.; Cleries, L.; Serra, P.; Ferrater, C.; Morena, J. L. *Thin Solid Films* **1998**, *317*, 393.
(15) Yoshimura, M.; Suchanek, W. *Solid State Ionics* **1997**, *98*, 197.
(16) Hata, K.; Kokubo, T.; Nakashi, N.; Yamamuro, T. *J. Am. Ceram. Soc.* **1995**, *78*, 1049.
(17) Tanahashi, M.; Yao, T.; Kokubo, T.; Minoda, M.; Miyamoto, T.; Nakamura, T.; Yamamuro, T. *J. Am. Ceram. Soc.* **1994**, *77*, 2805.
(18) Kokubo, T.; Miyaji, F.; Kim, H. *J. Am. Ceram. Soc.* **1996**, *79*, 1127.
(19) Reis, R. L.; Cunha, A. M.; Fernandes, M. H.; Correia, R. N. *J. Mater. Sci.: Mater. Med.* **1997**, *8*, 897.
(20) Li, S.; Liu, Q.; de Wijn, J.; Wolke, J.; Zhou, B.; de Groot, K. *J. Mater. Sci.: Mater. Med.* **1997**, *8*, 543.
(21) Layrolle, P.; Ito, A.; Tateishi, T. *J. Am. Ceram. Soc.* **1998**, *81*, 1421.
(22) Unuma, H.; Ito, K.; Ota, T.; Takahashi, M. *J. Am. Ceram. Soc.* **1996**, *79*, 2474.
(23) Fujishiro, Y.; Fujimoto, A.; Sato, T.; Okuwaki, A. *J. Colloid Interface Sci.* **1995**, *173*, 119.
(24) Nonami, T.; Taoda, H.; Hue, N. T.; Watanabe, E.; Iseda, K.; Tazawa, M.; Fukaya, M. *Mater. Res. Bull.* **1998**, *33*, 125.

10.1021/ja002537i CCC: $20.00
Published on Web 02/17/2001

Scheme 1. A Schematic Presentation of the Procedure To Prepare the Crystalline Dahllite Thin Films

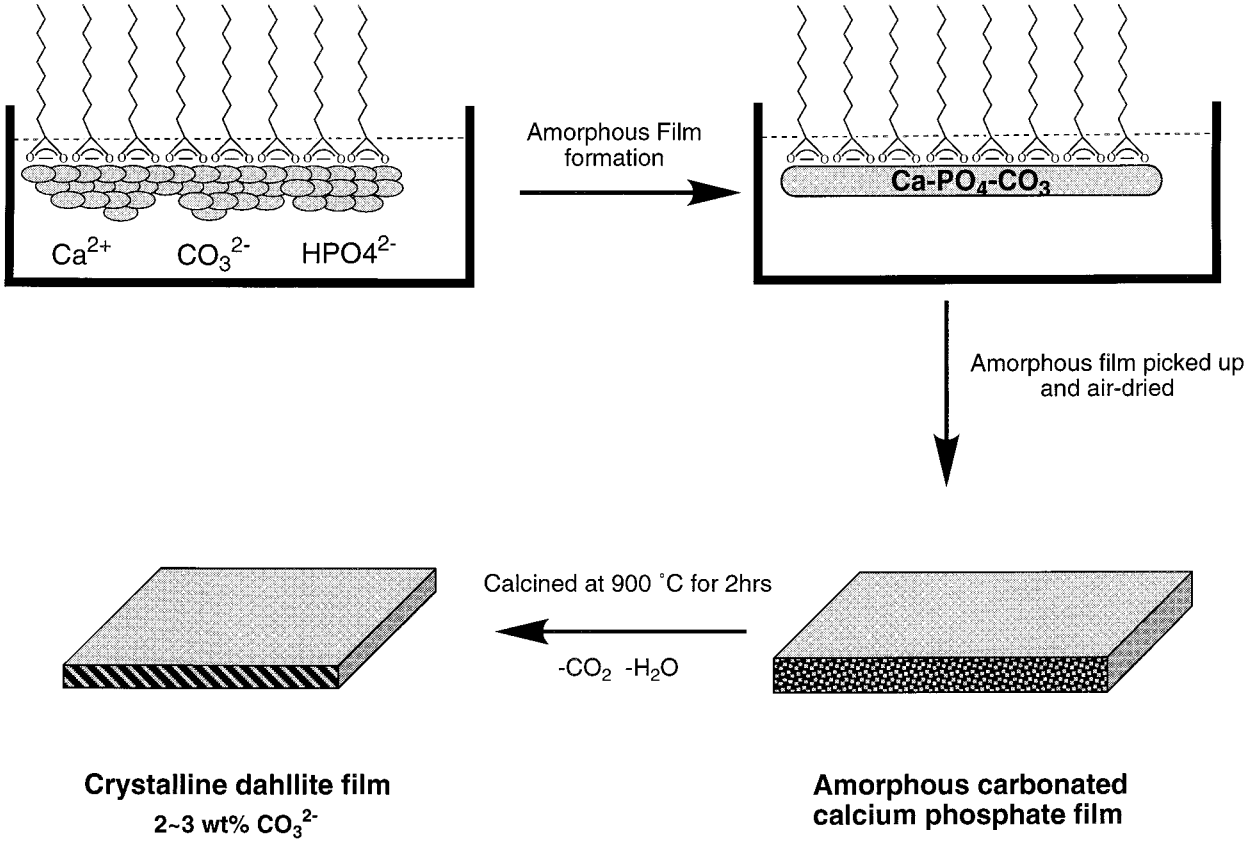

effort is still needed to improve the control over the crystallinity and the structure of the films.

Control over the structure and morphology of biological minerals has been exercised by many organisms with great elegance and accuracy. A few key mechanisms have been recognized for fulfilling this delicate control. One is the interplay between templating and inhibition of mineral growth. In this fashion, many sea shells have organized multiple layers of calcium carbonate in a highly ordered array in their nacres. Another strategy that has been utilized by organisms is an amorphous to crystalline transition.[25−27] In this process, an amorphous precursor forms first and then transforms into a crystalline phase while maintaining its morphology. Since an amorphous phase has a great flexibility in adapting complicated shapes, this phase transformation process can facilitate the formation of sophisticated structures. A good example is the formation of the sea urchin spicules,[28] in which an amorphous carbonate transforms into calcite. Another very important process of amorphous to crystalline phase transformation in biology was also identified in the carbonated calcium phosphate system. Lowenstam and Weiner illustrated a phase transformation process from amorphous calcium phosphate to crystalline dahllite in the formation of the radular teeth of chitons.[25] Certain synthetic amorphous carbonated calcium phosphates were also shown to transform directly into apatite crystal structure by heating.[1]

Recently, by mimicking the interplay between templates and inhibitors, we have developed a novel strategy to synthesize continuous thin films of calcium carbonate of macroscopic dimensions.[29,30] We have also shown that an amorphous to crystalline phase transformation can also be used to prepare ordered crystalline thin films of calcium carbonate in a biomimetic system.[29,31] In those studies, we used poly(acrylic acid) as the inhibitor to suppress the mineral formation in the bulk solution. Since both phosphate and carbonate are known to inhibit the crystal formation in a mutual fashion,[32,33] we propose that the template-inhibition method we have developed[29] can also be applied to the formation of the calcium carbonate phosphate system to produce amorphous calcium carbonate phosphate thin films. Crystallization of the precursor film can then be induced by either a hydrothermal[34,35] or a heating process[1] to yield crystalline thin films.

In this paper, we describe the synthesis of continuous dahllite thin films of macroscopic dimensions by this new synthetic strategy. An amorphous carbonated calcium phosphate thin film precursor was formed first, and followed by a heat-induced phase transformation to become a dahllite film (Scheme 1). A stearic acid monolayer formed at an air/subphase interface was used as a template to promote mineral deposition. The aqueous subphase was saturated calcium bicarbonate solution containing phosphate, which constituted a double-inhibition system.[32,33] On the one hand, phosphate ions strongly inhibited the nucleation

(25) Lowenstam, H. A.; Weiner, S. *Science* **1985**, *227*, 51.
(26) Lowenstam, H. A.; Weiner, S. *On Biomineralization*; Oxford University Press: Oxford, 1989.
(27) Mann, S. *Struct. Bonding (Inorg. Elements Biochem.)* **1983**, *54*, 125.
(28) Beniash, E.; Aizenberg, J.; Addadi, L.; Weiner, S. *Proc. R. Soc. London B* **1997**, *264*, 461.
(29) Xu, G.; Yao, N.; Aksay, I. A.; Groves, J. T. *J. Am. Chem. Soc.* **1998**, *120*, 11977.
(30) Lahiri, J.; Xu, G.; Yao, N.; Aksay, I. A.; Groves, J. T. *J. Am. Chem. Soc.* **1997**, *119*, 5449.
(31) Addadi, L.; Weiner, S. *Nature* **1999**, *398*, 461.
(32) Bachra, B.; Trautz, O.; Simon, S. L. *Arch. Biochem. Biophys.* **1963**, *103*, 124.
(33) Greenfield, D. J.; Eanes, E. D. *Calcif. Tiss. Inter.* **1972**, *9*, 152.
(34) Roy, D. M.; Linnehan, S. K. *Nature* **1974**, *247*, 220.
(35) Zaremba, C.; Morse, D. E.; Mann, S.; Hansma, P. K.; Stucky, G. D. *Chem. Mater.* **1998**, *10*, 3813.

and crystallization of calcium carbonate;[33] on the other hand, carbonate ions also prevented the formation of crystalline phosphate.[33] Further, the bicarbonate solution was a buffer system, which maintained a low solution pH to further suppress the precipitation of calcium phosphate. Thus, the formation of precipitates in the bulk solution was inhibited. However, the situation at the air−water interface was quite different and coprecipitation of both calcium carbonate and calcium phosphate was favored. Arrays of negatively charged acidic groups provided a template favorable for mineral deposition, which was coupled with a slightly higher pH and super-saturation degree due to the diffusion of CO_2 into the air. The balance between the templating and inhibition effects leads to a forced two-dimensional growth of the minerals at the air/water interface. This growth process resulted in a continuous thin film containing calcium salts of both carbonate and phosphate. A subsequent heat treatment of the film readily transformed it into a crystalline carbonate apatite film, which maintained the integrity of the film morphology.

Experiments and Methods

Subphase Preparation. Supersaturated $Ca(HCO_3)_2$ solution prepared according to an established procedure[29] was used as the aqueous subphase, which had a pH of 6.2 and calcium concentration of ~9 mM as determined from EDTA titration. A known amount of Na_3PO_4 from a stock solution of 0.2 M was mixed with the above $Ca(HCO_3)_2$ solution to reach a final concentration of phosphate in the range of 0.1 to 5 mM. The initial pH of the solution mixture increased from 6.2 to 6.6 with an increasing amount of phosphate added.

Film Formation. Immediately after the preparation of the above subphase, a chloroform solution of stearic acid (1 mg/mL) was added to the air/water interface to reach a full monolayer coverage. The amount of stearic acid added was calculated according to its mean molecular area and the open area of a crystal dish so that the resulting monolayer corresponded to a liquid-condense state. The whole setup was left unstirred for different periods of time until a visible film formed at the air/water interface. The precursor film was then picked up with a microscope cover slip and air-dried. The dried film was calcined at 900 °C in a stream of dry air (24 mL/min) for 2 h.

Film Characterization. A Philips XL-30 field-emission-gun (FEG) scanning electron microscope (SEM) operating at 10 KV was used to study the morphology of the films, which were sputter-coated with a layer of chromium about 10 nm thick. Energy disperse X-ray spectroscopy (EDS) was used to determine the elemental composition and distribution in the films. Atomic force microscope (AFM) images of the film surfaces were obtained in a tapping mode in air by a Nanoscope III unit from Digital Instrument. For powder X-ray diffraction analysis, films were collected and grounded into fine powders and applied to the surface of a zero-background quartz holder, and then scanned at 0.5 °C/min with a step size of 0.03°, by a Scintag XRD diffractometer with an operating voltage of 45 KV and an operating current of 40 mA. For infrared analysis, films ground into powders were pressed into KBr pellets and scanned at 2 cm^{-1} resolution with a Nicolet 730 FTIR instrument. Thermogravimetric analysis was performed by heating the films at 10 °C/min in a flow of air (24 mL/min) with an STA-1500 instrument. Quantitative Ca/P ratios were determined by inductively coupled plasma analysis (ICP).

Materials Analytical grade $CaCO_3$ (A.R., Mallinckrodt), Na_3PO_4 (A.R., Aldrich), stearic acid (A.R., Aldrich), and KBr (infrared grade, Aldrich) were used as obtained. Aqueous subphase was prepared from Milli-Q water.

Results

Preparation of the Precursor Film. The formation of a carbonated calcium phosphate precursor thin film took place underneath a liquid-condensed monolayer of stearic acid, which was deposited onto a calcium bicarbonate subphase containing phosphate. Depending on the starting phosphate concentration, the formation of a visible film took 3 to 8 h. Films formed faster with higher phosphate concentration and grew thicker over time. In a typical case, when a starting concentration of phosphate was 1.0 mM, thin films became visible after about 4 h and reached a thickness of ~1 μm after about 24 h. The films so formed were continuous, transparent, and smooth. During this period of time, the subphase remained clear and no precipitate was observed. By contrast, in the control experiments in which no stearic acid monolayers were used, the subphase appeared cloudy due to bulk precipitation, and no films were formed. Instead, patches of particulate aggregates were precipitated at the air/water interface (Figure 1c).

The phosphate thin films could be readily lifted up on a glass cover slip and dried in air. The air-dried films were also transparent and displayed iridescence. The areas of the films were in the order of several square centimeters. The free-standing films tended to curl upon drying. The dried films had considerable mechanical strength and could be handled with tweezers without breaking. Figure 1 shows the SEM image of an air-dried film prepared from a solution containing 1.0 mM phosphate. The cross-section of the film indicates a dense structure with a homogeneous thickness of about 1.2 μm. When viewed at a low magnification, both surfaces of the film were smooth. At higher magnification, the side originally facing the subphase appeared relatively rough and was covered with numerous small fused particles whose diameters were less than 100 nm (Figure 1b). The opposite side of the film, which originally faced the stearic acid monolayer, was smooth and featureless even at high magnification (Figure 1a). However, a closer examination of this smooth side with AFM indicated that it contained primary particles with diameters of 40−50 nm (Figure 1a, inset). Taken together, the above observations indicate that the film formed through a sequence of particle deposition and fusion process. Primary particles formed first directly under the acidic template and condensed into a thin layer, which acted as the template for the deposition and condensation of the next layer of particles. A continuation of this process resulted in a continuous film with micrometer thickness. This growth mechanism was also supported by the following observation. When a grown film was picked up and re-floated on top of another freshly prepared subphase, the growth process continued and the film got thicker, whereas the air/water interface of the subphase that was not covered with this mineral layer only yielded discrete particle aggregates, as observed in the control experiments (Figure 1c).

Elemental Analysis of the Precursor Film. The elemental composition of the films was examined by both EDS and ICP. Figure 2a shows the EDS spectrum of a film, which contained Ca, P, C, and O. The distribution of these elements was homogeneous across the film as examined by X-ray elemental mapping analysis (data not shown). The exact Ca/P molar ratio of the films was determined by ICP analysis and found to be dependent on the starting phosphate concentration of the subphase (Figure 3). At low phosphate concentrations, the Ca/P ratio was high due to the formation of an excess amount of calcium carbonate. The Ca/P ratio decreased as phosphate concentration increased until a plateau of 1.6 was reached at a phosphate concentration of about 0.8 mM. As the phosphate concentration was increased further, the Ca/P molar ratio of the film stayed relatively constant at 1.7 ± 0.1. In particular, films grown from a subphase containing 1.0 mM phosphate had a Ca/P molar ratio of 1.65 ± 0.06, very close to the Ca/P ratio of stoichiometry hydroxyapatite or carbonate apatite (dahllite). The

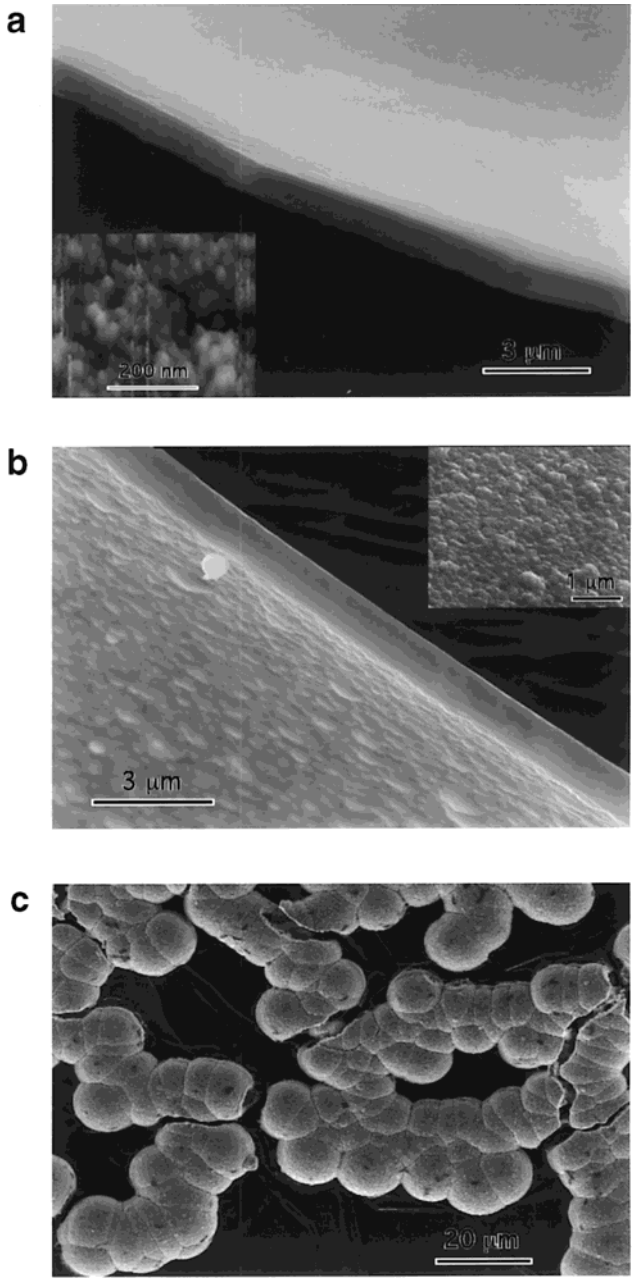

Figure 1. (a) SEM image of the carbonated calcium phosphate thin film precursor grown at the air/water interface, showing the side facing the stearic acid monolayer; inset is the AFM image of the same surface, the gray vertical stripes in the AFM image are scanning artifacts. (b) SEM image of the carbonated calcium phosphate thin film precursor grown at the air/water interface, showing the side facing the subphase; inset is the SEM image of the same surface at higher magnification. (c) In control experiments, aggregated particles formed in the absence of the stearic acid monolayer.

Ca/P ratio of biological apatite varies from 1.55 to 1.85, depending on both the species and the functions.[1,3] We also observed that films grown from the same subphase but for different periods of time had a similar Ca/P ratio (Figure 4). Since films grow thicker over time, this enables the preparation of films with similar composition but different thicknesses.

IR of the Precursor Film. The composition as well as the structure of the films was further investigated by infrared spectroscopy. Figure 5a shows the FT-IR spectrum of the films that have been air-dried and kept in a desiccator. The pattern of the absorption peaks is typical for hydrated carbonated

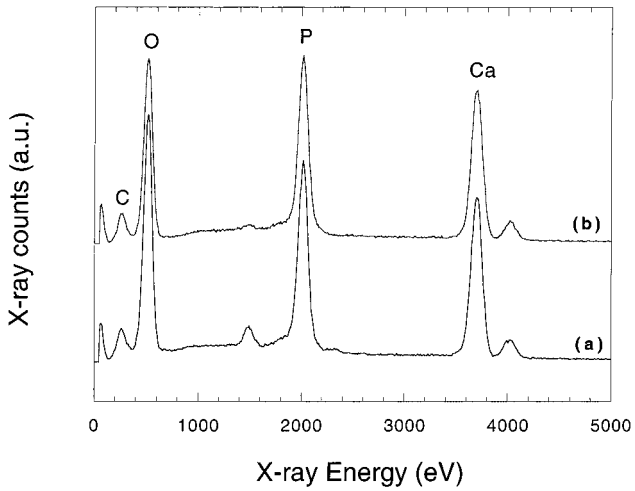

Figure 2. EDS spectra of (a) the carbonated calcium phosphate thin film precursor grown at the air/water interface and (b) the crystalline carbonate apatite film formed by a heat-treatment of the precursor film at 900 °C for 2 h.

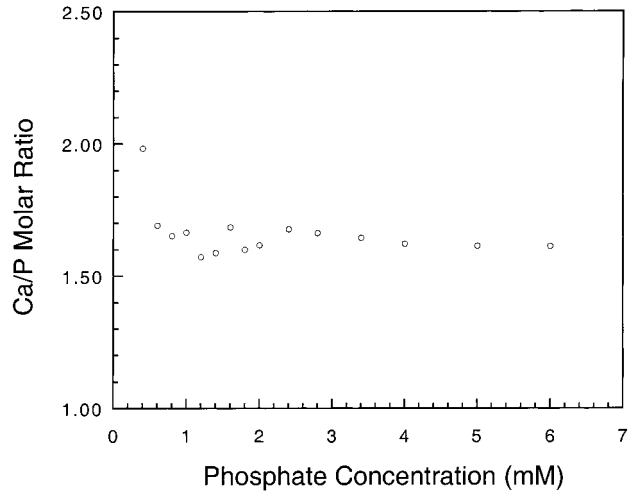

Figure 3. The relation between the calcium-to-phosphate molar ratio (Ca/P ratio) of the carbonated calcium phosphate thin films precursor and the starting phosphate concentration of the subphase.

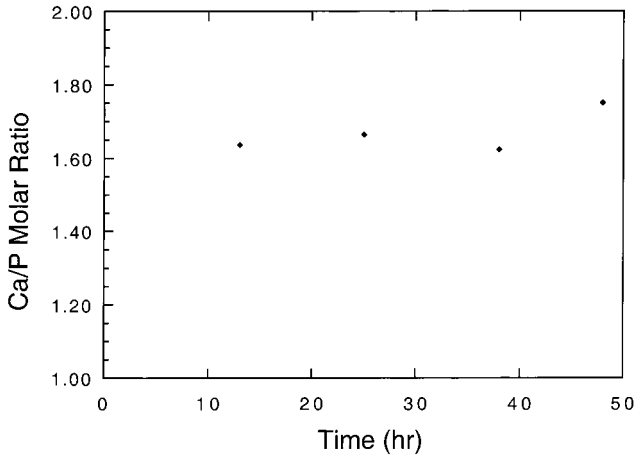

Figure 4. The relation between the calcium-to-phosphate molar ratio (Ca/P ratio) of the carbonated calcium phosphate thin film precursors and the growth time. The starting phosphate concentration was 1.0 mM.

calcium phosphate. The broad absorption bands around 3380 cm^{-1} and the bands between 1600 and 1650 cm^{-1} are due to incorporated water molecules.[36] The absorption bands at 1428

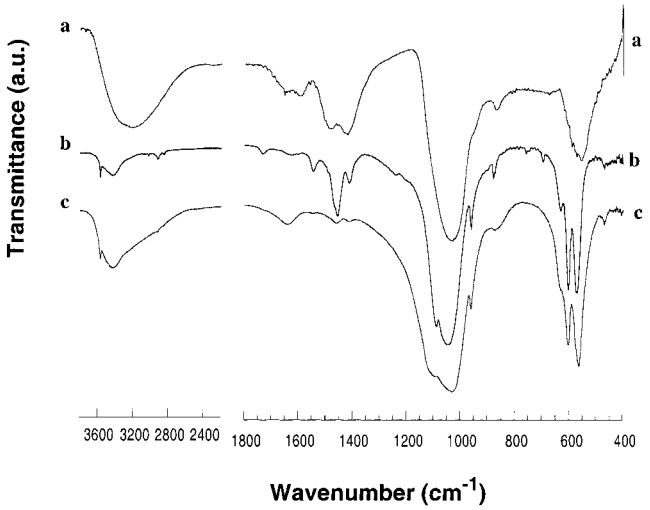

Figure 5. FT-IR spectra. (a) Air-dried precursor amorphous carbonated calcium phosphate thin films. The peaks at 3380, 1650, and 1600 cm^{-1} are due to incorporated water; the peaks at 1486, 1428 and 874 cm^{-1} are from the carbonate; the peaks at 1056 and 566 cm^{-1} are assigned to the phosphate. (b) Carbonate apatite crystalline films formed by the heat-treatment of the precursor films at 900 °C for 2 h. The peak assignments are as follows: 3572 and 632 cm^{-1} (OH stretch and liberation), 1546, 1456, and 880 cm^{-1} (υ_{3b}, υ_3, and υ_2 of CO_3^{2-} replacing OH^-, type A substitution), 1465, 1413, and 873 cm^{-1} (υ_{3b}, υ_{3a}, and υ_2 of CO_3^{2-} replacing PO_4^{3-}, type B substitution), 1045 and 1088 cm^{-1} (υ_3 of PO_4^{3-}), 962 cm^{-1} (υ_1 of PO_4^{3-}), 602 and 572 cm^{-1} (υ_4 of PO_4^{3-}). The assignments are based on refs 1 and 50. (c) Commercial hydroxyapatite.

and 1486 cm^{-1} come from υ_3 modes of the carbonate and are characteristic of a carbonate in an amorphous phase.[21,37] The υ_2 mode of carbonate also gives a sharp absorption at 874 cm^{-1}. Since this peak happens to overlap with the absorption from a P−O(H) stretching mode of possible HPO_4^{2-} ions,[36,38] it is difficult to quantify the amount of HPO_4^{2-} ions.[38,39] However, previous studies have shown that calcium phosphates precipitated under pH 8 and in the presence of carbonate contained HPO_4^{2-} ions.[33,38] Therefore, the presence of HPO_4^{2-} ions in the films cannot be excluded under the experiment conditions. The strong and broad bands centered at 1056 and 566 cm^{-1} are assigned to the υ_3 P−O stretching and υ_4 bending modes of the phosphate, respectively. The 1056 cm^{-1} band appears featureless, also indicating that the film contains an amorphous phase.[21,37] This agrees with the fact that no splitting in the 566 cm^{-1} band is observed, which is another indication of amorphous calcium phosphate.[37,40,41]

XRD of the Precursor Film. The amorphous nature of the films was also confirmed by powder X-ray diffraction (Figure 6a). No discerning diffraction peaks but two broad humps were observed at about 31° and 47° (2θ), which was characteristic of an amorphous phase. The dried films were very stable at room temperature. Typically, amorphous calcium phosphate is not very stable and can readily transform into the crystalline phase such as nonstoichiometry hydroxyapatite or tricalcium phosphate.[1] However, the presence of carbonate ions can significantly increased the stability of the amorphous phase

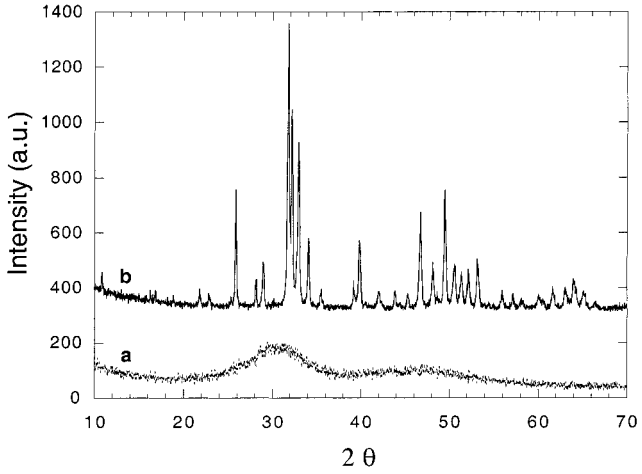

Figure 6. Powder XRD patterns of (a) air-dried precursor amorphous carbonated calcium phosphate thin films and (b) carbonate apatite crystalline films formed by the heat-treatment of the precursor films at 900 °C for 2 h.

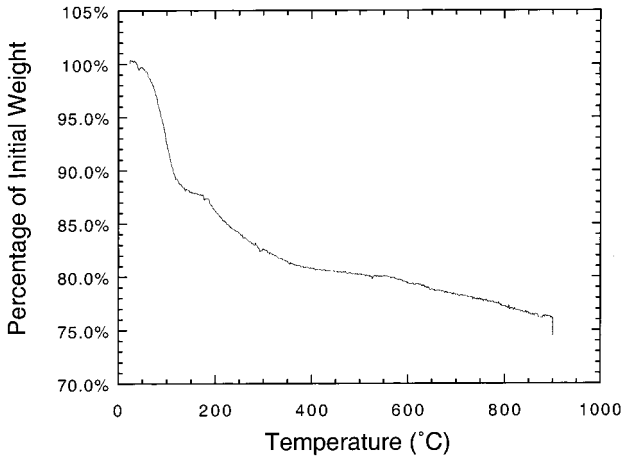

Figure 7. TGA curve of the carbonated calcium phosphate thin film precursor grown at the air/water interface. The films were heated at 10 °C/min in a flow of dry air and isothermed at 900 °C for 2 h. The vertical line at 900 °C reflects the weight loss of the sample due to the escape of CO_2 during the 2 h of isotherming at that temperature.

against conversion to the crystalline phase.[1,11,42−44] Hence, the stability of the amorphous films is attributed to the existence of a significant amount of carbonate ions.

Preparation of the Crystalline Dahllite Film. The morphology of the films was also very stable. After a period of several months, the shape of the films remained unchanged and no disintegration of the films was observed. The morphology of the films was stable even at high temperature. Heat treatment of the films at 900 °C for 2 h caused a shrinkage of about ∼16% in the film thickness, accompanied by a total weight loss of about 25% from the elimination of H_2O and CO_2 (Figure 7).[13,36,45,46] However, the integrity of the film morphology remained. The sintered film could still be handled with tweezers without breaking. Figure 8 compares the morphology of the films before and after the sintering at low (a and b) and high (c and d) magnification. The cross-sectional views (Figure 8c,d)

(36) Zhou, J.; Zhang, X.; Chen, J. *J. Mater. Sci.: Mater. Med.* **1993**, *4*, 83.
(37) Termine, D.; Lundy, D. L. *Calcif. Tiss. Res.* **1971**, *7*, 163.
(38) Apfelbaum, F.; Diab, H.; Mayer, I.; Featherstone, J. D. B. *J. Inorg. Biochem.* **1992**, *45*, 277.
(39) Apfelbaum, F.; Mayer, I.; Featherstone, J. D. B. *J. Inorg. Biochem.* **1990**, *38*, 1.
(40) Termine, J. D.; Posner, A. S. *Science* **1966**, *153*, 1523.
(41) Termine, J. D.; Posner, A. S. *Nature* **1966**, *211*, 268.
(42) Termine, J. D.; Peckauskas, R. A.; Posner, A. S. *Arch. Biochem. Biophys.* **1970**, *140*, 318.
(43) Posner, A. S.; Betts, F. *Acc. Chem. Res.* **1975**, *8*, 273.
(44) Blumenthal, N. C.; Holmes, J. M. *Calcif. Tiss. Res.* **1972**, *7*, 1181.
(45) Mayer, I.; Featherstone, J. D. B.; Nagler, R.; Noejovich, M.; Deutsch, D.; Gedalia, I. *J. Solid State Chem.* **1985**, *56*, 230.
(46) Takahashi, H.; Yashima, M.; Kakihana, M.; Yoshimura, M. *Eur. J. Solid State Inorg. Chem.* **1995**, *32*, 829.

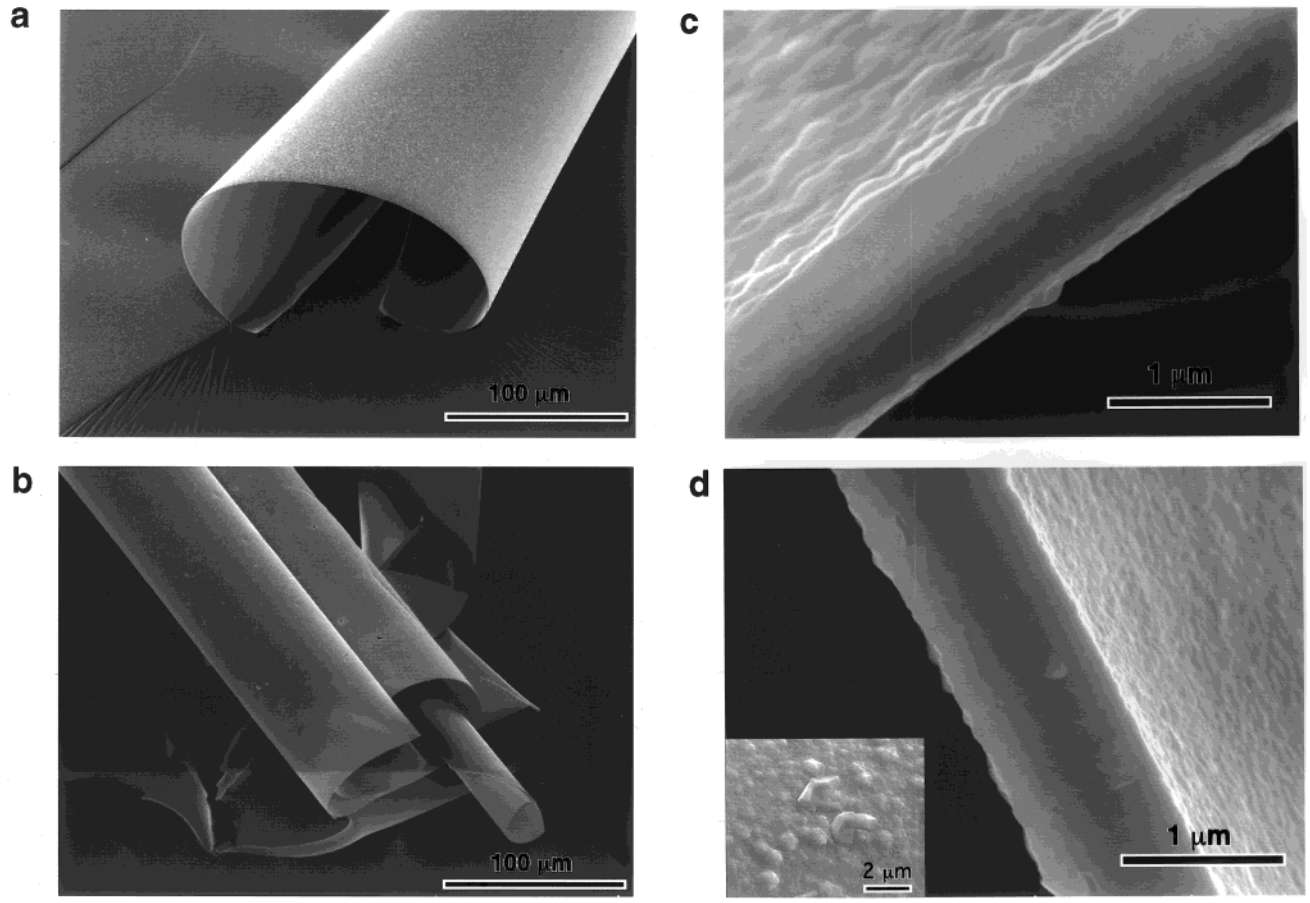

Figure 8. (a) Low magnification SEM image of the carbonated calcium phosphate thin film precursor before the heat treatment. (b) Low magnification SEM image of the carbonated calcium phosphate thin film after the heat treatment at 900 °C for 2 h. (c) High magnification SEM image of the carbonated calcium phosphate thin film precursor before the heat treatment, showing the cross-section of the film. (d) High magnification SEM image of the carbonated calcium phosphate thin film precursor after the heat treatment at 900 °C for 2 h, showing the cross-section of the film (inset: top view).

show that the film remained dense after the heat treatment. The original flat surface became slightly rougher, while the roughness of the other surface decreased due to the heat treatment. The overall shape of the films was largely unchanged.

Although the overall morphology of the films underwent little change, the microstructure of the films had transformed from the amorphous phase into a polycrystalline apatitic phase. The formation of the crystalline phase was also noticeable from the appearance of faceted crystallites on the film surface (Figure 8d, inset). The structure of the crystalline films was determined by both XRD and FT-IR to be an AB-type carbonated hydroxyapatite.

XRD of the Dahllite Film. Figure 6b shows the powder XRD pattern of the crystalline films and Table 1 lists the corresponding diffraction peak index and intensity. The parameters of the apatite hexagonal unit cell were determined from the diffraction peaks to be 9.409 and 6.886 Å for *a*-axis and *c*-axis, respectively. The formation of a single apatite phase was attributed to the fact that the Ca/P molar ratio of the precursor film was very close to that of crystalline apatite.[1,36,46]

Because the loss of either Ca or P was unlikely in the temperature range at which the film was heat-treated, the Ca/P molar ratio of the crystalline film should stay the same as its precursor.[21,36] This was confirmed by EDS analysis of the films before and after the heat treatment (Figure 2). In both cases, the relative intensity of calcium and phosphorus was the same, indicating the Ca/P molar ratio was unchanged. The content of CO_3^{2-} in the carbonate apatite can be estimated from the reduction of its *a*-axis relative to that of hydroxyapatite, since the replacement of PO_4^{3-} by CO_3^{2-} causes shortening of the *a*-axis.[1,6,7] Using the literature value of the *a*-axis dimension (9.426 Å) for nonsubstituted hydroxyapatite[47] and the reported relationship between *a*-axis and CO_3^{2-} content,[1,6,7,48,49] the content of the CO_3^{2-} in the crystalline film was estimated to be ∼2 wt %.

IR of the Dahllite Film. The change of both the crystal structure and the composition of the film after the heat treatment was also indicated by the change of its infrared absorption pattern.[1,50] The FTIR spectra of the crystalline film and a commercial hydroxyapatite are shown in Figure 5, parts b and c, respectively. Compared with the precursor film (Figure 5a), the crystalline film has sharp and well-resolved peaks at 950∼1100 and 550∼650 cm^{-1}, characteristic of a well-crystallized apatite phase. The peaks at 1088 and 1046 cm^{-1} are assigned to υ_3 stretching of PO_4^{3-}, and the peaks at 962 and 476 cm^{-1} are assigned to υ_1 stretching and υ_2 bending modes of PO_4^{3-}, respectively. There are two well-separated peaks at 602 and 572 cm^{-1}, both assigned to the υ_4 mode of PO_4^{3-}. The large separation of these two peaks is another indicator of a highly crystallized apatitic phase.[40,41,51]

(47) Simpson, D. R. *Science* **1965**, *147*, 501.
(48) Bocchi, G.; Valdre, G. *J. Inorg. Biochem.* **1993**, *49*, 209.
(49) Trombe, J.; Bonel, G.; Montel, G. *Bull. Soc. Chim. Fr.* **1968**, 1708.
(50) Fowler, B. O. *Inorg. Chem.* **1974**, *13*, 194.
(51) LeGeros, R. Z. *Calcium Phosphate in Oral Biology and Medicine*; Karger: Basel, Switzerland, 1991.

Table 1. Indexed *d* spacing (in hexagonal unit cell) of the X-ray Diffraction Result of the Films Calcined at 900 °C for 2 h[a]

h	*k*	*l*	*d*(obsd), Å	*d*(calcd), Å
2	0	0	4.071	4.074
1	1	1	3.885	3.884
0	0	2	3.440	3.442
1	0	2	3.169	3.171
2	1	0	3.080	3.080
2	1	1	2.811	2.811
1	1	2	2.778	2.778
3	0	0	2.717	2.716
2	0	2	2.629	2.629
3	0	1	2.527	2.527
2	1	2	2.295	2.295
3	1	0	2.260	2.260
3	1	1	2.147	2.147
1	1	3	2.062	2.062
2	0	3	2.000	1.999
2	2	2	1.943	1.942
3	1	2	1.890	1.891
2	1	3	1.841	1.840
3	2	1	1.804	1.804
4	1	0	1.778	1.778
4	0	2	1.753	1.753
0	0	4	1.721	1.721
3	1	3	1.611	1.610
5	0	1	1.585	1.586
2	1	4	1.503	1.502
5	0	2	1.473	1.473
3	0	4	1.453	1.454
5	1	1	1.431	1.432

[a] $a = 9.4089$ Å. $c = 6.8843$ Å. $\gamma = 120°$. Cell volume = 527.8021 Å^3.

The IR absorption peaks in the regions at 1400−1600 cm^{-1} and 860−880 cm^{-1} are due to the CO_3^{2-} ions in the apatite lattice and the positions of these peaks are sensitive to the substitution environment of the CO_3^{2-} ions.[1,4,49] There are two types of substitution sites for CO_3^{2-} ions in an apatite lattice, commonly known as type A and type B substitution. Type A substitution refers to CO_3^{2-} ions replacing OH^- ions in the 6-folded screw axis; while type B substitution refers to CO_3^{2-} ions replacing PO_4^{3-} ions.[1,4,49] The IR spectrum of the crystalline film has peaks at 1465, 1413, and 873 cm^{-1}, which are assigned to the υ_{3b}, υ_{3a}, and υ_{3b} modes of B-type CO_3^{2-} ions.[1,4,49] The spectrum also contains peaks at 1546, 1465 (as a shoulder), and 880 cm^{-1}, which are assigned to υ_{3b}, υ_{3a}, and υ_{3b} modes of A-type CO_3^{2-} ions.[1,4,49] Thus, the CO_3^{2-} ions in the crystalline film resided in both A-type and B-type sites. However, the substitution of OH^- by CO_3^{2-} was incomplete, as indicated by the OH^- peaks at 3572 and 698 cm^{-1}. The content of the B-type CO_3^{2-} in the crystalline film can be calculated by the ratio of the extinction of the 1413 cm^{-1} peak (CO_3^{2-}) to that of the 573 cm^{-1} peak (PO_4^{3-}).[45,52,53] It was estimated to be ∼2 wt %, which agreed well with the carbonate content determined from the X-ray diffraction data.

Discussions

It is worth noting that the true carbonate content of the crystalline film was actually higher than the value obtained above since both the IR and X-ray methods used were primarily for B-type carbonate apatite. Hence, the total carbonate content was underestimated.[48] In the case of the CO_3^{2-} estimation by lattice parameter (XRD), A-type CO_3^{2-} ions also contributed to the change of *a*-axis, but in the opposite way. Thus, it offset some of the *a*-axis reduction due to B-type CO_3^{2-} ions. In the case of the CO_3^{2-} estimation by IR absorption, the 1413 cm^{-1} peak was only from B-type CO_3^{2-} ions and, therefore, the content of A-type CO_3^{2-} was not included.

However, the content of A-type CO_3^{2-} can be roughly estimated by the following methods. The first method uses the ratio of the extinction of the 1546 cm^{-1} peak (A-type CO_3^{2-}) to that of the 1413 cm^{-1} peak (B-type CO_3^{2-}), assuming that these two peaks have a similar extinction coefficient.[54] Alternatively, the residual OH^- content can be calculated by comparing the ratio (α) of the extinction of the 3571 cm^{-1} peak (OH^-) to that of the 573 cm^{-1} peak (PO_4^{3-}) with the corresponding ratio of nonsubstituted hydroxyapatite.[54,55] This calculation is also based on an assumption that a linear relationship exists between the ratio (α) of the extinctions and the OH^- content. The amount of A-type CO_3^{2-} can then be estimated by subtracting the residual OH^- content from the total OH^- content in a stoichiometric hydroxyapatite lattice. The above two analyses were applied to the crystalline film and similar results were obtained in both cases. There was ∼1 wt % A-type carbonate in the films.

However, these semiquantitative estimations should be taken with caution because of the inherent errors due to the existence of several substitution mechanisms by carbonate ions[56] and subsequent overlaps of the infrared absorption peaks in these wavenumber regimes. Therefore, more rigorous methods are needed to accurately determine the total carbonate content. Nevertheless, the crystal structure of the film can be described as a carbonate apatite, with carbonate substitution in both OH^- (type A) and PO_4^{3-} (type B) lattice positions and with a total carbonate concentration of 2−3 wt %. It is worth pointing out that many biological apatites also contain both type-A and type-B carbonate with a similar total concentration.[1]

Although the carbonated apatite films we synthesized had a carbonate content similar to that of biological apatites, the two types of apatites are different in several aspects. First, the biological apatites are formed in physiological conditions while the synthetic apatites were prepared at high temperature. Second, biological apatites, often in the shape of small needles or flakes, exist as a highly structured three-dimensional composite with organic matrix. The synthetic apatite film is a pure inorganic and two-dimensional structure. Third, the biological apatites are usually poorly crystallized or exist as microcrystallites, which often gives rise to broad X-ray diffraction peaks. The synthetic apatite, on the other hand, was well crystallized.

Previous studies on amorphous calcium phosphate showed that in the presence of carbonate, the amorphous-to-apatitic transformation could take place at a temperature as low as 500−600 °C.[1,46] Therefore, the precursor carbonated calcium phosphate thin films we have synthesized can be thermally processed to form crystalline carbonate apatite in a wide temperature range (500−900 °C). The degree of crystallinity of the heat-treated films can be tuned by controlling the processing temperature and time. Further, the carbonate content of the heated films is also influenced by a number of factors including the starting carbonate content, temperature, and the duration of the heat treatment.[13] Since these parameters are all adjustable, the strategy we have developed can be used to produce a spectrum of carbonated apatite thin films with a variety of thicknesses,

(52) Featherstone, J. D. B.; Pearson, S.; LeGeros, R. Z. *Caries Res.* **1984**, *18*, 63.
(53) Arends, J.; Davidson, C. L. *Calcif. Tiss. Res.* **1975**, *18*, 65.
(54) Driessens, F. C. M.; Woltgens, J. H. M.; Verbeeck, R. M. H. *Bull. Soc. Chim. Belg.* **1984**, *93*, 161.
(55) Verbeeck, R. M. H.; Driessens, F. M. C.; Borggreven, J. M. P. M.; Woltgens, J. H. M. *Bull. Soc. Chim. Belg.* **1985**, *94*, 237.
(56) Pieters, H. Y.; DeMaeyer, E. A. P.; Verbeeck, R. M. H. *Inorg. Chem.* **1998**, *37*, 6392.

crystallinity, and carbonate content. The two-dimensional morphology and the smoothness of these free-standing films make them viable to serve as models for studying the interactions of biological mineral surface with biological entities, such as cell-mineral adhesions and protein-crystal interactions.

Conclusions

We have demonstrated a novel biomimetic strategy for synthesizing continuous macroscopic-scale films of both amorphous carbonated calcium phosphate and crystalline carbonate apatite. The thin films of amorphous carbonated calcium phosphate were prepared by the "template-inhibition" method. The amorphous films were rich in carbonate and had a Ca/P molar ratio of ~1.66. The crystalline dahllite thin films were prepared by a heat treatment of the amorphous films at 900 °C for 2 h. The crystalline films were determined to be a single phase carbonate apatite, with carbonate substitution in both OH^- (type-A) and PO_4^{3-} (type-B) lattice positions and a total carbonate content of 2−3 wt %. During the heat treatment, the overall shape of the films was maintained.

Acknowledgment. Support of this research by the Princeton Materials Institute and National Science Foundation (NSF) is gratefully acknowledged. We thank Edward Vicenzi for the assistance in AFM operation and Maria Borscic for ICP measurements.

JA002537I